PB90-233305

Acceleration by Pulsar Winds in Binary Systems

(U.S.) National Aeronautics and Space Administration, Albuquerque, NM

30 Jan 90

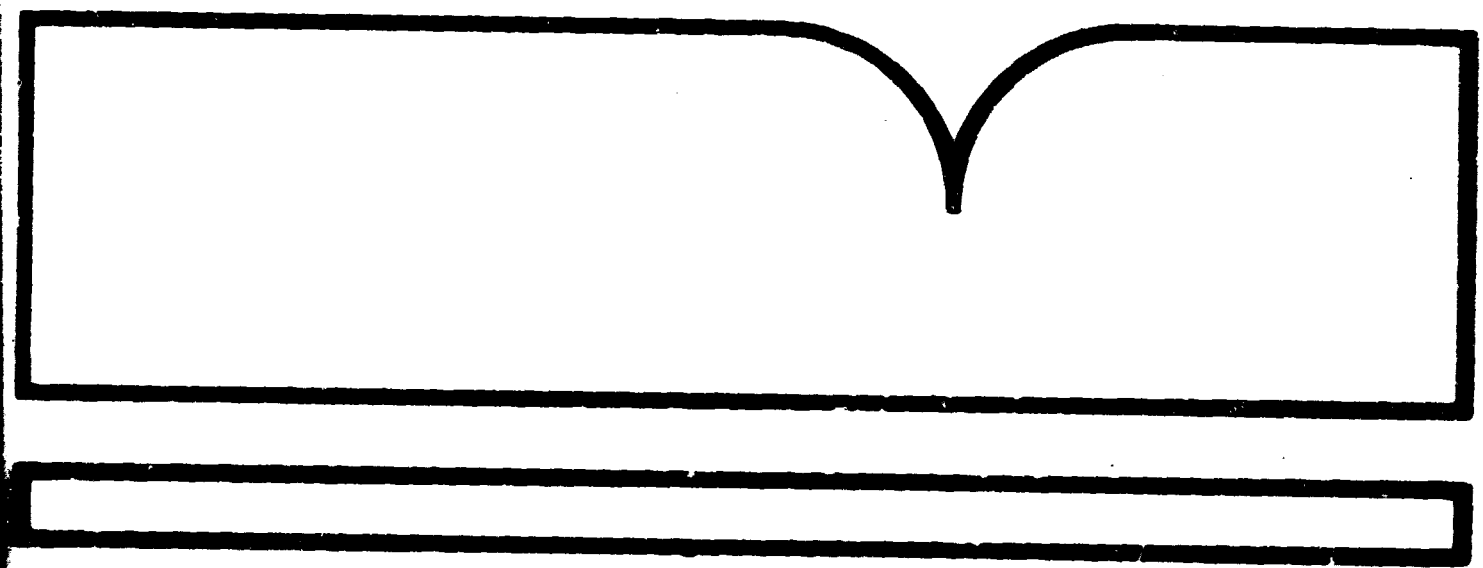

BIBLIOGRAPHIC INFORMATION

PB90-233305

Report Nos: none

Title: Acceleration by Pulsar Winds in Binary Systems.

Date: 30 Jan 90

Authors: A. K. Harding, and T. K. Gaisser.

Performing Organization: National Aeronautics and Space Administration, Albuquerque, NM. Lab. for High Energy Astrophysics.**Franklin Inst., Newark, DE. Bartol Research Foundation.

Supplementary Notes: Also available from Supt. of Docs. Prepared in cooperation with Franklin Inst., Newark, DE. Bartol Research Foundation.

NTIS Field/Group Codes: 54C

Price: PC A03/MF A01

Availability: Available from the National Technical Information Service, Springfield, VA. 22161

Number of Pages: 43p

Keywords: Binary stars, *Pulsars, *Stellar winds, *Particle acceleration, Proton acceleration, Astronomical models, Gamma ray astronomy, Cygnus X-3 X ray source.

Abstract: In the absence of accretion torques, a pulsar in a binary system will spin down due to electromagnetic dipole radiation and the spin-down power will drive a wind of relativistic electron-positron pairs. Winds from pulsars with short periods will prevent any subsequent accretion but may be confined by the companion star atmosphere, wind or magnetosphere to form a standing shock. The authors investigate the possibility of particle acceleration at such a pulsar wind shock and the production of VHE and UHE gamma rays from interactions of accelerated protons in the companion star's wind or atmosphere. They find that in close binaries containing active pulsars, protons will be shock accelerated to a maximum energy dependent on the pulsar spin-down luminosity. If a significant fraction of the spin-down power goes into particle acceleration, these systems should be sources of VHE and possibly UHE gamma rays. The authors discuss the application of the pulsar wind model to binary sources such as Cygnus X-3, as well as the possibility of observing VHE gamma-rays from known binary radio pulsar systems.

ACCELERATION BY PULSAR WINDS IN BINARY SYSTEMS

Alice K. Harding

and

T. K. Gaisser

LABORATORY FOR HIGH ENERGY ASTROPHYSICS

LHEA

National Aeronautics And Space Administration

Goddard Space Flight Center

Greenbelt, Maryland 20771

Acceleration By Pulsar Winds in Binary Systems

Alice K. Harding
Laboratory for High Energy Astrophysics
NASA/Goddard Space Flight Center

and

T.K. Gaisser
Bartol Research Institute
University of Delaware

January 30, 1990

To appear in the Astrophysical Journal,
August 1, 1990 issue

Abstract

In the absence of accretion torques, a pulsar in a binary system will spin down due to electromagnetic dipole radiation and the spin-down power will drive a wind of relativistic electron-positron pairs. Winds from pulsars with short periods will prevent any subsequent accretion but may be confined by the companion star atmosphere, wind or magnetosphere to form a standing shock. We investigate the possibility of particle acceleration at such a pulsar wind shock and the production of VHE and UHE gamma rays from interactions of accelerated protons in the companion star's wind or atmosphere. We find that in close binaries containing active pulsars, protons will be shock accelerated to a maximum energy dependent on the pulsar spin-down luminosity. If a significant fraction of the spin-down power goes into particle acceleration, these systems should be sources of VHE and possibly UHE gamma rays. We discuss the application of the pulsar wind model to binary sources such as Cygnus X-3, as well as the possibility of observing VHE γ-rays from known binary radio pulsar systems.

I. Introduction

Magnetized, non-accreting neutron stars will spin down through energy losses due primarily to magnetic dipole radiation (Ostriker and Gunn 1969). Since the observed radiation from pulsars at radio frequencies and above accounts for only a small fraction of their total spin down energy loss, it was originally proposed that the bulk of this energy is carried away in the form of large amplitude electromagnetic waves at the rotation frequency of the pulsar. The development of pulsar models since the work of Ostriker and Gunn has shown that vacuum conditions outside the star cannot exist in the presence of electric forces many times the gravitational force at the stellar surface (Goldreich and Julian 1969). Furthermore, it is very likely that pair production takes place somewhere in the pulsar magnetosphere (Sturrock 1971), raising the particle density in these regions to several orders of magnitude above the corotation charge density. Under these conditions, the plasma frequency at the light cylinder will be significantly higher than the frequency of the dipole radiation (see e.g. Arons 1981). Consequently, the dipole electromagnetic waves cannot propagate and the pulsar spin-down energy will most likely be transported by a relativistic MHD wind consisting mostly of electron-positron pairs (Rees and Gunn 1974).

Confinement of pulsar winds can occur if there exists enough pressure surrounding the pulsar to balance the wind ram pressure. The static pressure of the interstellar medium is not large enough to confine the wind of an isolated pulsar. However, if the pulsar is surrounded by a supernova remnant or is moving relative to the interstellar medium, then the wind can be confined. In their model for the Crab nebula, Rees and Gunn (1974) proposed that the expanding shell would confine the pulsar wind at a standing shock where the wind ram pressure balances the total magnetic field and particle pressure in the nebula. They assumed that since the field and particles in the nebula have come from the pulsar (the present field in the Crab nebula is many times larger than the remnant field of the expanded stellar envelope), the nebular pressure results from the energy accumulated over the pulsar's lifetime. Kennel and Coroniti (1984a,b) have extended the ideas of Rees and Gunn to construct a detailed pulsar wind model of the Crab nebula. Cheng (1983) has considered the confinement of pulsar winds by ram pressure from the pulsar's motion through the interstellar medium. In this case a bow shock forms ahead of the star at the pressure balance point and the synchrotron radiation from the shocked wind particles is predicted to

be observable in X-rays. A bow shock of this kind may have been observed in Hα emission surrounding PSR1957+20 (Kulkarni and Hester 1989).

In this paper, we consider the possibility of confinement of a pulsar wind by a binary companion. Pulsar winds in binaries were investigated by Davies and Pringle (1979) and were first proposed as a model for Cygnus X-3 by Bignami *et al.* (1973). More recently, the interaction of a pulsar wind with a binary companion has been considered in models for the evolution of low-mass X-ray binaries (Ruderman, Shaham and Tavani 1989, Ruderman *et al.* 1989), in particular for the eclipsing 1.6 ms pulsar PSR1957+20 (Phinney *et al.* 1988, Kluzniak *et al.* 1988, Cheng 1989). In Section II, we discuss the conditions under which pulsar winds can form in binary systems and the confinement of the pulsar wind either by gas or magnetic pressure in the companion star atmosphere or by the ram pressure of the companion star wind. In both cases, the location of the stationary shock front relative to the separation of the two stars is calculated. In Section III, we explore the possibility of first order Fermi acceleration of charged particles by the pulsar wind shock and estimate the energy to which the particles can be accelerated. The high energy gamma rays resulting from interactions of these particles with material in the companion star atmosphere is discussed in Section IV. In Section V we discuss the application of these results to binary sources such as Cygnus X-3 which have been observed in UHE and VHE gamma rays, as well as the possibility of observing this type of emission from known binary pulsar systems.

II. Formation of the Pulsar Wind Shock

The power in magnetic dipole radiation from a pulsar with rotation frequency Ω and magnetic dipole moment m is

$$L_d = \frac{2m^2\Omega^4 \sin^2\theta}{3c} \approx 4 \times 10^{43}\,\mathrm{erg\,s^{-1}}\, B_{12}^2 P_{ms}^{-4} \qquad (1)$$

where P_{ms} is the period in ms, $B_{12} = (B_o/10^{12}\mathrm{Gauss})$ is the surface magnetic field and θ is the angle between the dipole and rotation axes. We assume that all of this power appears as a relativistic wind which carries both particles (predominantly electron-positron pairs) and wound-up magnetic field away from the pulsar. Since the magnetic field is dipolar ($\approx r^{-3}$) inside the pulsar light cylinder, $r_{LC} = c/\Omega = 5 \times 10^6\,\mathrm{cm}\, P_{ms}$, and toroidal ($\approx r^{-1}$) in the

wind, the field strength at a distance r is

$$B = B_o(\frac{r_o}{r_{LC}})^3(\frac{r_{LC}}{r}) = 8 \times 10^9 \text{Gauss}\, B_{12} P_{\rm ms}^{-3}(\frac{r_{LC}}{r}), \quad (2)$$

where $r_o = 10^6$ cm is the neutron star radius. Eqn (2) implicitly assumes equipartition between magnetic field energy and particle energy in the wind (Auriemma, Gaisser and Lipari 1988). Winds from pulsars with short periods have higher magnetic fields because the light cylinder, inside which the field falls off most rapidly, is closer to the neutron star.

Accretion onto the neutron star will not take place as long as the pulsar light cylinder, r_{LC}, where the wind would be generated, is inside the Alfven radius, $r_A = 1.5 \times 10^8 \text{ cm}\, B_{12}^{4/7} \dot{M}_{18}^{-2/7}$. This will be the case for pulsars with periods

$$P < 31 \text{ ms}\, B_{12}^{4/7} \dot{M}_{18}^{-2/7}, \quad (3)$$

where $\dot{M}_{18} = \dot{M}/10^{18} \text{g s}^{-1}$ is the accretion rate (see also Ruderman, Shaham and Tavani 1989). In these cases where the light cylinder is inside the Alfven radius, the ram pressure from the wind, $L_d/4\pi r^2 c$, everywhere exceeds the ram pressure of the accretion flow, ρv^2. In order to have a stable force balance between the pulsar wind and the accretion flow, ρv^2 must fall off with r more slowly than the $1/r^2$ dependence of the pulsar wind. For spherical accretion, $\rho v^2 \approx 1/r^{5/2}$, while for disk accretion, both in α disk (Shakura and Sunyaev 1973) and thick disk models ρv^2 falls off faster than $1/r^2$. Hence, there can be no confinement of the pulsar wind by an accretion flow. In fact, if the pulsar light cylinder is inside the Alfven radius, there can be no accretion flow at all since the pulsar wind is capable of blowing away accreting material at all radii (except where the companion star dominates the gravitational potential).

In the absence of an accretion flow, there are several other possibilities for confining the pulsar wind in a binary system, at least over a limited solid angle. We consider three general cases: 1) confinement by the static atmosphere of the companion where the gas pressure balances the ram pressure of the pulsar wind 2) confinement by the companion star wind where ram pressure of the two winds balance 3) confinement by the companion star magnetosphere.

In the second case, the wind from the companion star may be driven either by processes intrinsic to the companion or by the relativistic wind from neutron star (or by a combination of the two). Figure 1 shows a schematic representation of the pulsar wind shock formation.

A reverse shock will form on the pulsar side of the contact discontinuity which separates the pulsar wind from the companion star wind (or atmosphere) at the pressure balance point. We propose that particles may be accelerated at this shock. A reverse shock in the companion wind (as shown in Fig. 1 of Phinney *et al.* 1988) may also form if the wind speed becomes supersonic, but as pointed out by Cheng (1989), need not exist in all cases. The extent to which field line reconnection occurs in the shocked pulsar wind will probably depend on the geometry of the pulsar wind flow around the companion and could be an additional source of accelerated particles.

a) Companion Star Atmosphere

In the case of a static atmosphere, $L_d/(4\pi r^2 c)$ is balanced by the gas pressure, $\rho kT/m_{\rm H}$, close to the companion star so that the shock distance from the pulsar, $r = r_s \approx a - r_*$. In an isothermal atmosphere, the density has an exponential dependence, $\rho = \rho_o \exp(-z/h)$, so that significant changes in density occur over distances comparable to the scale height $h = kT/m_{\rm H}g$. To determine the density near the shock, we need to know the temperature in the atmosphere. A rough estimate may be obtained from requiring that the temperature be high enough to radiate away the pulsar wind power absorbed by the star, $L_* = \epsilon L_d$, where

$$\epsilon = \frac{\Omega_*}{4\pi} = \frac{1}{2}[1 - (1 - \frac{r_*^2}{a^2})^{1/2}]. \tag{4}$$

and Ω_* is the solid angle subtended by the companion. This condition, $S_*\sigma T^4 = \epsilon L_d$, where $S_* = 2\pi r_*^2(1 - r_*/a)$ is the area of the companion which can absorb wind power, gives the following temperature and scale height:

$$T = 2.2 \times 10^6\,{\rm K}\, B_{12}^{1/2} P_{\rm ms}^{-1} (\frac{R_\odot}{r_*})^{1/2} \frac{\epsilon^{1/4}}{(1 - r_*/a)^{1/4}} \tag{5}$$

$$h = 5.9 \times 10^9\,{\rm cm}\, B_{12}^{1/2} P_{\rm ms}^{-1} (\frac{r_*}{R_\odot})^{3/2} (\frac{M_\odot}{M}) \frac{\epsilon^{1/4}}{(1 - r_*/a)^{1/4}} \tag{6}$$

where a is the sum of semi-major axes of the binary system (i.e. the separation of the stars), and M and r_* are the companion star mass and radius. The atmospheric density at the discontinuity is then determined by the force balance condition to be

$$\rho_s = 1.2 \times 10^{-4}\,{\rm g\,cm^{-3}}\, B_{12}^{3/2} P_{\rm ms}^{-3} (\frac{R_\odot}{r_*})^{3/2} \frac{\epsilon^{-1/4} (r_*/a)^2}{(1 - r_*/a)^{7/4}}. \tag{7}$$

b) Companion Star Wind

In the case where the pulsar wind is confined by a stellar wind from the companion, we balance $L_d/(4\pi r^2 c)$ with $(\rho v^2)_w = \dot{M}_w v_w/(4\pi r^2)$. The shock radius is thus determined by

$$\frac{L_d}{4\pi r_s^2 c} = \frac{\dot{M}_w v_\infty}{4\pi(a-r_s)^2}\left[1-\frac{r_*}{a-r_s}\right]^{1/2}, \tag{8}$$

where $\dot{M}_w$ and v_∞ are the mass loss rate and terminal velocity of the wind, and r_s is the distance of the shock from the neutron star (cf. Fig. 1). Note that Eqn (8) is valid only for shock radii well outside the critical point radius, where the wind speed equals the local sound speed.

From Equation (8), $(\rho v^2)_w$ reaches a maximum value at $r_{max} = a - \frac{5}{4}r_*$. The condition that $(\rho v^2)_w$ balance the pulsar wind somewhere between the two stars, and thus the requirement for pressure balance, is $(\rho v^2)_{max} > L_d/4\pi r_{max}^2 c$ or from Eq. (8)

$$\left(\frac{a}{r_*}-\frac{5}{4}\right)^2 \left(\frac{r_*}{R_\odot}\right)^{-1/2} \dot{M}_{18}\left(\frac{v_\infty}{v_{esc}}\right)\left(\frac{M}{M_\odot}\right)^{1/2} B_{12}^{-2} P_{ms}^4 > 7\times 10^7, \tag{9}$$

where $v_{esc} = (2GM/r_*)^{1/2}$ is the escape velocity from the companion. If Eqn (9) is satisfied then Eqn (8) gives a solution to the shock radius r_s and we require that $r_{LC} < r_s < a - r_*$. Figure 2 shows the location of the shock from numerical solution of equation (8) as a function of r_*/a. In the limit $r_s << a - r_*$, the approximate analytic solution is

$$\frac{r_s}{a} \approx \frac{\sqrt{A_w}}{1+\sqrt{A_w}} \tag{10}$$

$$A_w = \frac{L_d}{\dot{M}_w v_w c} = \frac{2\times 10^7 B_{12}^2 P_{ms}^{-4}\left(\frac{r_*}{R_\odot}\right)^{1/2}}{\dot{M}_{18}\left(\frac{v_\infty}{v_{esc}}\right)\left(\frac{M}{M_\odot}\right)^{1/2}}. \tag{11}$$

The quantity A_w is essentially the ratio of pulsar wind ram pressure to stellar wind ram pressure and is therefore the critical parameter determining solutions for r_s.

From mass flux conservation, the stellar wind density near the discontinuity is

$$\rho_s = 2.64\times 10^{-13}\mathrm{cm}^{-3}\,\frac{\dot{M}_{18}\left(\frac{v_{esc}}{v_\infty}\right)\left(\frac{r_*}{a}\right)^2\left(\frac{M}{M_\odot}\right)^{-1/2}\left(\frac{r_*}{R_\odot}\right)^{-3/2}}{\left[1-\frac{r_*/a}{(1-r_s/a)}\right]^{1/2}(1-r_s/a)^2}, \tag{12}$$

where we have used the approximate solution of Eq. (10).

In the case where the stellar wind is driven by the companion star's self-generated radiation pressure, $\dot{M}_w$ and v_∞ are free parameters. In the case where the stellar wind is

induced by absorption of pulsar wind luminosity, solutions are almost completely defined by the pulsar wind power, which determines the ram pressure of both winds. We consider two special cases of pulsar-induced winds.

1. Radiation Pressure Driven Induced Winds

The pulsar wind power absorbed by the companion star, $L_* \approx \epsilon L_d$ is greater than the Eddington limit, $L_{\rm Edd} = 4\pi GcM/\kappa$, when

$$\epsilon B_{12}^2 P_{\rm ms}^{-4} \left(\frac{M_\odot}{M}\right) \left(\frac{\kappa}{\kappa_e}\right) > 3.15 \times 10^{-6}, \tag{13}$$

where κ is the opacity (with $\kappa_e = 0.4\,{\rm cm}^2/{\rm g}$ the electron scattering opacity) and ϵ is defined in Eqn (4).

If $\epsilon L_d > L_{Edd}$, then heating by the pulsar wind can drive a wind from the companion through radiation pressure. The wind terminal velocity will be

$$v_\infty = [2GM(\Gamma - 1)/r_*]^{1/2}, \tag{14}$$

where $\Gamma = \epsilon L_d \kappa / 4\pi GMc$ is the ratio of the radiation pressure force to the gravitational force. The induced mass loss can be estimated by the condition $\frac{1}{2}\dot{M}_I v_\infty^2 = \epsilon L_d$ (assuming that all of the absorbed energy goes into bulk kinetic energy of the wind with terminal velocity v_∞). In the limit $\Gamma >> 1$,

$$\dot{M}_{\rm I} = \frac{4\pi c r_*}{\kappa} = 6.6 \times 10^{22}\,{\rm g\,s^{-1}} \left(\frac{\kappa_e}{\kappa}\right) \left(\frac{r_*}{R_\odot}\right), \tag{15}$$

and $\dot{M}_{\rm I}$ is independent of L_d. If the opacity driving the wind comes mostly from lines, as is often the case in stellar atmospheres (Mihalis 1978, Castor *et al.* 1975), then κ may be much higher than the electron scattering opacity. Effects of self-shielding by the stellar wind may also reduce $\dot{M}_{\rm I}$ (Eichler and Ko 1988). Equations (14) and (15) give

$$\dot{M}_{18} \left(\frac{v_\infty}{v_{\rm esc}}\right) = 3.7 \times 10^7 P_{\rm ms}^{-2} B_{12} \left(\frac{M_\odot}{M}\right)^{1/2} \epsilon^{1/2} \left(\frac{\kappa_e}{\kappa}\right) \left(\frac{r_*}{R_\odot}\right). \tag{16}$$

Figure 3 shows numerical solutions of Eqn (8) for the shock location r_s, using Eqn (16) in the expression (11) for A_w. In the limit $r_s << a - r_*$, the variation of r_s/a in Fig. 3 comes from the ϵ dependence, which reflects the relative amount of pulsar wind power absorbed by the companion. The solutions shown in Fig. 3 must also satisfy $\epsilon L_d > L_{\rm Edd}$. Some $\dot{M} = \dot{M}_{\rm I}$

solutions may be unstable in the sense that $\dot{M}_1$ could be large enough to turn off the pulsar wind if the Alfven radius of the induced mass accretion onto the neutron star is inside the pulsar light cylinder, violating Eq (3). It is difficult to give a simple condition for systems with stable solutions, since the relation between the accretion rate $\dot{M}$ and the stellar mass loss rate $\dot{M}_w$ depends on the geometry of the system, wind angular momentum, etc.

2. Thermally Driven Winds

If $\epsilon L_d < L_{\rm Edd}$, the pulsar may still induce a wind from the companion star if the pulsar wind can efficiently heat the atmosphere to a temperature at which the mean particle velocity exceeds escape velocity. Kinetic energy gained by particles in the atmosphere can be converted directly to wind kinetic energy if the expansion time is less than the radiation (bremsstrahlung) timescale. Thermal wind models have been studied in the context of accreting sources where thermal X-rays from the neutron star drive a self-sustaining wind from the companion star. London, McCray and Auer (1981) and London and Flannery (1982) have shown that the resulting mass loss from X-ray heating is approximately

$$\dot{M} \simeq 5 \times 10^{-11} {\rm g\,s^{-1}}\, \phi^{-1/2} {\rm L_X}, \tag{17}$$

where $\phi = GM/r_* = v_{\rm esc}/2$ is the surface gravitational potential and L_X is the X-ray luminosity incident on the companion. Substituting this expression into Eqn (11) and assuming $v_w = v_{\rm esc}$, the parameter A_w which determines the shock radius becomes

$$A_w = \frac{0.466}{\epsilon} \approx 1.87 \left(\frac{a}{r_*}\right)^2 \tag{18}$$

where we have taken $L_X = \epsilon L_d$.

Thermally driven winds may also occur in some of the radio pulsar binary systems. Cheng (1989) has investigated a self-consistent model for pulsar-induced stellar winds, in which the estimated mass loss rate from the companion is given (from his Eqn [17]) by,

$$\dot{M} = P_* \left(\frac{GM}{r_*}\right)^{-1/2} \gamma_c (\zeta\delta)^{1/2} \left(\frac{\zeta\delta}{\mu}\right)^{\mu} A_o \tag{19}$$

where P_* is the pulsar wind ram pressure, A_o is the cross sectional area at the base of the wind flow ($\approx \pi r_*^2$), $\zeta = (v_\infty/v_{\rm esc})^2$ and μ, γ_c and δ are dimensionless parameters specifying the flow geometry. From the above expression (with $\mu = 1.5, \gamma_c = 5/3, \delta = 0.5$,), we can

derive the product of mass-loss rate and terminal velocity,

$$\dot{M}_{18}\left(\frac{v_\infty}{v_{esc}}\right) = 1.7\times 10^6 B_{12}^2 P_{ms}^{-4}\left(\frac{v_{esc}}{v_\infty}\right)^3\left(\frac{r_*}{R_\odot}\right)^{1/2}\left(\frac{M_\odot}{M}\right)^{1/2}\left(\frac{r_*}{a}\right)^2. \qquad (20)$$

Inserting the above expression into Eqn (11) gives a particularly simple form for the parameter A_w which determines the shock location:

$$A_w = 11.5\left(\frac{v_\infty}{v_{esc}}\right)^3\left(\frac{a}{r_*}\right)^2 \qquad (21)$$

Solutions for r_s as a function of r_*/a are therefore dependent only on the wind terminal velocity. Figure 4 shows numerical solutions of Eqn (8) for the shock location in the thermal wind model of Cheng (1989) as a function of r_*/a and (v_∞/v_{esc}). The solutions are constrained by Eqn (9) to require

$$\left(\frac{v_\infty}{v_{esc}}\right) \le 0.29\left(1-\frac{5r_*}{4a}\right)^{2/3} \qquad (22)$$

in the limit that the shock radius lies well outside the critical point.

c) Companion Star Magnetosphere

If the companion star has a surface magnetic field, B_*, then magnetic pressure may be sufficient to stand off the pulsar wind. In this case, the shock location can be found by balancing $[B_*(r_s)]^2/8\pi$ with $L_d/(4\pi r_s^2 c)$. Assuming a dipole field, r_s is determined by

$$\frac{B_*^2}{8\pi}\left(\frac{r_*}{a-r_s}\right)^6 = \frac{L_d}{4\pi r_s^2 c} \qquad (23)$$

Solutions for the shock location from Eqn (23) are determined by the quantity

$$A_m = \frac{2L_d}{B_*^2 a^2 c}, \qquad (24)$$

which scales with the ratio of pulsar wind ram pressure to magnetic pressure. Figure 5 shows numerical solutions for r_s from Eqn (23) as a function of the parameter A_m. The condition that the shock form above the companion star surface, or $(a-r_s)\ge r_*$, requires that $A_m \le (1-r_*/a)^2 \le 1$, which from Eqn (24) gives a limit on the companion star field capable of standing off the pulsar wind,

$$B_* \ge \left(\frac{2L_d}{c}\right)^{1/2}\frac{1}{(a-r_*)}. \qquad (25)$$

III. Shock Acceleration of Particles

Once a shock forms in the pulsar wind as a result of confinement, the conditions may be favorable for first-order Fermi acceleration of particles. Shock acceleration has gained considerable attention recently as a mechanism for generating highly energetic particles in a variety of sources which include supernovae (Lagage and Cesarsky 1983), the interstellar medium (Blandford and Ostriker 1978), the Earth's bow shock (Ellison and Eichler 1984), stellar winds from hot stars (Cesarsky and Montmerle 1983) and pulsar winds in supernova remnants (Gaisser, Harding and Stanev 1987, 1989). If the shock is formed by collisionless processes, particles can travel back and forth across the shock front by scattering from magnetic irregularities, gaining some energy on each crossing. The spectrum of accelerated particles escaping downstream is a power law with index dependent on the shock compression ratio. The theory of diffusive shock acceleration (cf. Drury 1983 for review) has concentrated primarily on strong parallel shocks (where the magnetic field is parallel to the shock normal), in which the jump conditions lead to a compression ratio

$$\xi = \frac{u_1}{u_2} = \frac{4}{1 + 3/\mathcal{M}^2} \rightarrow 4. \tag{26}$$

Here $\mathcal{M}$ is the Mach number of the shock. The standard treatment also is for non-relativistic shocks for which $u_1, u_2 \ll c$. Such a shock produces a power law spectrum with index of the differential energy spectrum $\alpha = 2 + 4/\mathcal{M}^2$.

The shock in the relativistic pulsar wind differs from the canonical case in two ways. First, because of the toroidal field, the shock is quasi-perpendicular rather than parallel, so that the jump conditions require compression of the magnetic field across the shock. This actually tends to increase the acceleration rate because the particles spend more time in the vicinity of the shock and gain energy by drifting through the potential drop induced along the shock (Jokipii, 1987). Second, the pulsar wind shock is relativistic in that the velocity of the unshocked wind relative to the shock front is $u_1 \approx c$. Treatments of acceleration by relativistic shocks (Peacock 1981; Kirk and Schneider 1987) indicate that they are more efficient at accelerating particles than non-relativistic shocks (the energy gain per crossing is larger). Recent Monte-Carlo simulations of Ellison, Jones and Reynolds (1990) give a shorter acceleration time in relativistic shocks and show that the accelerated particle spectrum is flatter than for a non-relativistic shock with the same compression ratio. However, the resulting spectral index is somewhat uncertain, since the two approximations usually made to

treat scatterings in the non-relativistic case, pitch angle scattering or hard-sphere scattering, give different results in the relativistic case.

For the present, we simply assume that this configuration of a relativistic shock with a quasi-perpendicular field configuration is capable of accelerating particles at least as efficiently as the non-relativistic, parallel shock. We then use the well developed theory of non-relativistic, parallel shocks to estimate the acceleration rate and hence the maximum energy accessible. The acceleration rate for a relativistic particle is (Lagage and Cesarsky 1983)

$$\dot{E} \approx \frac{1}{3\xi}\frac{(\xi-1)}{(\xi+1)}\frac{u_1^2 E}{D}, \tag{27}$$

where D is the diffusion coefficient (which we assume to be the same both upstream and downstream) and u_1 is the flow velocity of the upstream (unshocked) fluid into the shock. We now use the minimum value of the diffusion coefficient to obtain an upper limit on the acceleration rate and hence an upper limit on the maximum energy that can be achieved. We take $D_{\rm min} = r_L v/3$, where $r_{\rm L} = 3.3 \times 10^9 {\rm cm}\, E_{\rm TeV}/B$ is the Larmor radius, v is the particle velocity, and E is the particle energy. For $u_1 \approx c \approx v$ the resulting estimate of the acceleration time is

$$t_a \approx \frac{E}{ceB}\frac{\xi(\xi+1)}{(\xi-1)}. \tag{28}$$

Because of the inverse dependence on field strength, which from Eq (2) is large, and the relativistic velocity of the wind, the pulsar wind shock is extremely efficient at accelerating particles to high energy.

a) Conditions for Shock Acceleration

The conditions under which diffusive shock acceleration can take place are 1) the plasma must have $\beta < 1$, where $\beta \equiv B_s^2/4\pi\gamma\rho c^2$ is the ratio of magnetic to particle energy density in the plasma. This condition is necessary for the existence of a strong shock (Kennel and Coroniti 1984a) and also for the development of magnetic turbulence which scatters the particles 2) the shock must be collisionless, forming as a result of magnetic turbulence or other collective plasma effects rather than by collisions of individual particles, i.e. the plasma and photon densities both upstream and downstream of the shock must be low enough to prevent inelastic collisions from dominating the scattering.

The first condition is equivalent to requiring that the Alfven velocity be less than the

particle velocity, which for relativistic flows is close to c. Kennel and Coroniti (1984a) and Emmering and Chevalier (1987) have examined relativistic pulsar wind solutions as a model for the Crab nebula. In these models the solutions are constrained by matching the jump conditions at the shock and by the expansion velocity of the shell which confines the wind. The free parameter, σ, characterizing the flow solutions in these models is the ratio of the magnetic energy flux to particle energy flux in the unshocked wind and thus is the same as the parameter β defined above. The value of σ (or β) in a pulsar wind is not well determined, because there exists no global solution which relates the particle production in the pulsar magnetosphere and flow of these charged particles through the light cylinder with the wind solutions outside. Large values of σ, where the flow is highly magnetized, produce weak shocks with low thermalization, while small values of σ give a strong MHD shock approaching the classical hydrodynamic limit. The above studies find that a very small value of σ ($\approx 10^{-3}$) is required to match the present expansion rate and synchrotron luminosity of the Crab nebula. There are indications therefore that pulsar winds have $\beta < 1$, favorable for shock acceleration. If particle energy flux dominates magnetic energy flux in a pulsar wind, then the strength of the magnetic field at the shock would be lower than that derived by assuming equipartition (Eqn [2]) by a factor of $\sigma^{\frac{1}{2}}$, reducing the acceleration energy by the same factor.

The second condition requires that the mean free path for inelastic scattering or absorption processes be large compared to the acceleration length, $l_a = ct_a$. To examine whether the second condition is satisfied in the pulsar wind, we will consider both nuclear collisions and photo-pion production in the radiation field of the companion. The nuclear collision mean free path is $l_{pp} \approx \lambda_{pp}/\rho$, where $\lambda_{pp} \approx 60\,\mathrm{g\,cm^{-2}}$ is the interaction length in H at around 1 TeV (λ_{pp} decreases slowly with energy to a value of $35\,\mathrm{g\,cm^{-2}}$ at 150 TeV). The ratio of l_{pp} to the the acceleration length, using the pulsar wind density ρ determined by the value of β, t_a from Eqn (28) and magnetic field from Eqn (2), is

$$\frac{l_{pp}}{l_a} = 3.7 \times 10^8 \gamma \beta B_{12}^{-1} P_{ms}^2 E_{TeV}^{-1} \left(\frac{r_*}{R_\odot}\right) \left(\frac{a}{r_*}\right) \left(\frac{r_*}{a}\right) \frac{(\xi - 1)}{\xi(\xi + 1)} \qquad (29)$$

Thus, the requirement $l_{pp} > l_a$ gives an upper limit on the proton energy E_{TeV}. Since it is expected that $\gamma >> 1$, possibly as large as 10^6 (Kennel and Coroniti 1984a), this limit will not be important in most cases.

Protheroe (1983) has studied pair production and photopion production by $> 10^{12}$ eV

protons in UHE sources and gives attenuation times in blackbody radiation fields of $T_{BB} \approx 10^4 - 10^5$ K from the stellar companion. The attenuation times for photopion production, important for protons with $E > 10^{15}$ eV, range from $\approx 10^2\,\mathrm{s}\,(T_{BB} = 8 \times 10^4$ K) to $\approx 10^6\,\mathrm{s}\,(T_{BB} = 10^4$ K) and attenuation times for pair production vary from $\approx 10^4 - 10^8$ s for the same temperature range. With the shock velocity $u_1 \approx c$, as in the case of a relativistic pulsar wind and the magnetic field from Eqn (2), the strong shock acceleration time from Eq. (28), $t_a = 10^{-6}\,\mathrm{s}\,E_{\mathrm{TeV}} B_{12}^{-1} P_{ms}^2 (r_s/10^{11}$ cm), is very short compared to the attenuation times above, even for energies $> 10^{18}$ eV.

b) Maximum Acceleration Energy

The maximum energy to which (charged) particles can be accelerated in the shock is determined by the balance of the energy gain rate with losses. The time t_a needed for the shock to accelerate particles to an energy E was given in Eqn (28). The energy gains of the particles crossing the shock compete with energy losses through radiation and inelastic collisions and with diffusion away from the shock. For protons, diffusion is the dominant loss process since radiative losses are negligible even at the higher energies. Synchrotron losses are unimportant in limiting the maximum proton energy in nearly all cases (see below). The time to diffuse a distance r is $t_d = r^2/D$, where D is the diffusion coefficient and r is usually taken to be the shock radius. Equating the acceleration time, t_a, to the diffusion timescale t_d gives the maximum acceleration energy. With the minimum value of D, the maximum proton energy is

$$E_p^{\max} \approx \sqrt{\frac{3(\xi - 1)}{\xi(\xi + 1)}}\, e B_s r, \tag{30}$$

where the characteristic energy $e B_s r \approx 10^7$ TeV $B_{12} P_{ms}^{-2}$ in the case where $r = r_s$. Requiring the particle gyroradius to be less than the shock radius results in the same limit, to within a factor of 2 or 3. The maximum energy $E_p^{\max}$ is approximately equal to the potential drop across the pulsar polar cap, $\phi_p = e r_o^3 \Omega^2 B_o / c$. Because ϕ_p also equals the potential drop across the shock, the same $E_p^{\max}$ would result from drift acceleration in the perpendicular case. The electron acceleration will be limited by synchrotron losses, so their maximum energy is determined by equating the acceleration time in Eqn (28) to the synchrotron loss timescale.

1. Static atmosphere

In the case of a shock in a static isothermal atmosphere, the proton energy will be limited by diffusion downstream into denser parts of the atmosphere where collisions become dominant. The scale length for diffusion is therefore the atmospheric scale height h rather than the shock radius $r \approx r_* >> h$. The condition determining the maximum acceleration energy is therefore $t_a = t_d \approx h^2/D$. With the shock velocity $u_1 = c$, the magnetic field from Eqn (2) evaluated at r_s and scale height from Eq. (6), the maximum proton energy is

$$E_p^{\max} = 1.02 \times 10^6 \,\mathrm{TeV} \sqrt{\frac{3(\xi-1)}{\xi(\xi+1)}}\, B_{12}^{3/2} P_{\rm ms}^{-3} \left(\frac{r_*}{R_\odot}\right)^{1/2} \left(\frac{r_*}{a}\right) \left(\frac{M_\odot}{M}\right) \epsilon^{1/4} (1 - r_*/a)^{5/4} \qquad (31)$$

The electron maximum energy is limited by synchrotron radiation losses whose timescale is $t_s = 200\, s\, B^{-2} E_{\rm TeV}^{-1}$. Equating this timescale to the acceleration time t_a and taking the magnetic field from Eqn (2), the maximum electron energy is

$$E_e^{\max} = .033\,\mathrm{TeV}\, B_{12}^{-1/2} P_{\rm ms} \left(\frac{a}{r_*}\right)^{1/2} \left(\frac{r_*}{R_\odot}\right)^{1/2} \left(1 - \frac{r_*}{a}\right)^{1/2} \sqrt{\frac{3(\xi-1)}{\xi(\xi+1)}} \qquad (32)$$

Figure 6 shows the regions of parameter space defined by Eqs. (13), (29) and (31) where a strong ($\xi = 4$) pulsar wind shock in a stellar atmosphere could accelerate protons to energies above 10 and 10^4 TeV. The limits have been plotted for $M/M_\odot = r_*/R_\odot = \kappa/\kappa_e = 1$, although the dependence of the L_d limits on these quantities is not very strong. There is a very restricted, but finite, parameter space (defined by the shaded strip) where protons can be accelerated above 10 TeV and no parameters for which acceleration to 10^4 TeV is possible. The general conclusion is that protons up to around 10 TeV can be produced by a pulsar wind shock which forms due to confinement by the atmosphere of the companion in a close binary.

2. Stellar wind or magnetosphere

In the case of confinement by a stellar wind or magnetosphere, the diffusion length scale which determines the maximum proton energy depends on how close the pulsar wind shock is to the companion star. If $r_s << a - r_*$, then the radius of the shock will be approximately r_s and $t_d = r_s^2/D$, but if $r_s \approx a - r_*$ with the shock near the companion star, then the shock radius will be approximately $a - r_s$ and $t_d = (a - r_s)^2/D$. The maximum proton energy in

these two cases is

$$E_p^{\max} = 1.2 \times 10^7 \,\mathrm{TeV}\, B_{12} P_{\rm ms}^{-2} \sqrt{\frac{3(\xi-1)}{\xi(\xi+1)}} \begin{cases} 1, & r_s << a - r_* \\ \left(\frac{a}{r_s} - 1\right), & r_s \approx a - r_* \end{cases} \tag{33}$$

Note that in the case $r_s << a - r_*$, the r_s dependence in $E_p^{\max}$ (cf. Eqn [30]) drops out, because $B_s \propto 1/r_s$, so that the maximum proton acceleration energy depends only on pulsar parameters. In fact, $E_p^{\max} \propto L_d^{1/2}$. The synchrotron loss timescale for protons, $t_s = 5 \times 10^{15}\, s\, B^{-2}\, E_{\rm TeV}^{-1}$, is a factor $(m_p/m_e)^4$ longer than for electrons. The maximum energy obtained by equating the synchrotron loss timescale to the acceleration time in Eqn (28) is lower than the maximum energy given in Eqn (33) when $P_{\rm ms}\, B_{12}^{-1/2}\, (r_s/R_\odot)^{1/6} < 3.6$. Thus, synchrotron losses are important in limiting the proton acceleration energy only in the case of millisecond pulsars with high magnetic fields. These pulsars, if they exist, would have spin-down timescales of $10 - 100$ yr.

As before, the maximum electron energy is determined by the balance of acceleration time and synchrotron loss time, but in the stellar wind case depends on the location of the shock:

$$E_e^{\max} = .033\,\mathrm{TeV}\, B_{12}^{-1/2} P_{\rm ms} \left(\frac{a}{r_*}\right)^{1/2} \left(\frac{r_*}{R_\odot}\right)^{1/2} \left(\frac{r_s}{a}\right)^{1/2} \sqrt{\frac{3(\xi-1)}{\xi(\xi+1)}} \tag{34}$$

The general conclusion here is that a pulsar wind shock due to confinement by a stellar wind (regardless of whether or not it is induced by the pulsar wind heating) or magnetosphere is capable of accelerating protons to energies of 10 TeV if $P_{\rm ms} B_{12}^{-1/2} < 900$ and 10^4 TeV if $P_{\rm ms} B_{12}^{-1/2} < 30$. These limits translate, from Eq. (1), into pulsar wind power limits of $L_d > 6 \times 10^{31}$ erg/s and $L_d > 5 \times 10^{37}$ erg/s. As mentioned in Section IIb, induced wind solutions where $\dot{M}$ is large enough that the Alfven radius is inside the pulsar light cylinder would be unstable. These unstable solutions would occur for longer period pulsars with large light cylinder radii. If the accretion rate from the stellar mass loss is around the Eddington limit, then the requirement for a stable solution from Eqn (3) would be $P_{\rm ms} B_{12}^{-4/7} < 31$. This requirement would essentially restrict the parameter space to only those systems capable of accelerating protons to 10^4 TeV.

IV. High Energy Gamma-Ray Emission

Protons accelerated at the pulsar wind shock could produce γ-rays and neutrinos by decay of pions, which would result when the protons interact with surrounding material (or con-

ceivably with ambient photons if their density is high enough). The protons that diffuse away from the shock are no longer confined in the pulsar wind and can cross the contact discontinuity to reach the companion star or other target material. Photons produced in interactions in the companion star wind or atmosphere would likely be modulated at the orbital period. If the shock is near the companion then the target subtends a relatively large solid angle at the proton source region around the pulsar wind shock (see Fig. 1). This model therefore may have a higher efficiency for converting accelerated proton luminosity into γ-rays than models in which protons are accelerated at the compact object. In the latter case the target subtends a much smaller solid angle at the proton source.

The production spectrum of photons at the source is given by a convolution of the differential spectrum of accelerated protons, $\phi_p(E_p) = K\,E_p^{-\alpha}$, with the target density, the production cross section for π^0's and the π^0 decay spectrum (Gaisser, 1988). Explicitly, the rate of photon production per target H atom is

$$\frac{\mathrm{d}n_\gamma}{\mathrm{d}E_\gamma} = 2\int_{E_\gamma}^{E_p^{\max}} \mathrm{d}E_p \int_{E_\gamma}^{E_p} \frac{\mathrm{d}E_\pi}{E_\pi^2}\, f(x)\, \phi_p(E_p). \tag{35}$$

Here $x \equiv E_\pi/E_p$, and the momentum distribution of pions produced when protons collide in hydrogen is given by

$$\frac{\mathrm{d}n_{p\to\pi^0}}{\mathrm{d}E_\pi} = \frac{f(x)}{E_\pi}.$$

The extra factor of $2/E_\pi$ in Eqn (35) comes from the photon distribution in $\pi^0 \to 2\gamma$. The accelerator is assumed to produce a power law spectrum of protons (differential index α) with a sharp cutoff at maximum energy $E_p^{\max}$.

One integration by parts leads to

$$\frac{\mathrm{d}n_\gamma}{\mathrm{d}E_\gamma} = \frac{2\,K}{\alpha(E_\gamma)^\alpha}\left\{\int_{x_\gamma}^1 (z^\alpha - x_\gamma^\alpha)\, f(z)\,\frac{\mathrm{d}z}{z^2}\right\}, \tag{36}$$

where $x_\gamma \equiv E_\gamma/E_p^{\max}$. A similar manipulation gives an expression for the integral spectrum of photons as

$$N_\gamma(>E_\gamma) = \frac{2\,K}{\alpha(\alpha-1)}\frac{1}{(E_\gamma)^{\alpha-1}} Z_{p\pi^0}(x_\gamma), \tag{37}$$

where

$$Z_{p\pi^0}(x_\gamma) \equiv \int_{x_\gamma}^1 \left[(z^\alpha + (\alpha-1)x_\gamma^\alpha) - z\alpha(x_\gamma)^{\alpha-1}\right] f(z)\frac{\mathrm{d}z}{z^2}. \tag{38}$$

The function $f(x)$ is determined by accelerator data. Berezinsky & Kudryavtsev (1989) give an explicit expression which we use for numerical calculations:

$$f(x) = 0.61\,(1-x)^{3.5} + 0.46\,\exp(-18x). \tag{39}$$

In the high energy limit ($x_\gamma \to 0$), the function $Z_{p\pi^0}(x_\gamma)$, plotted in Figure 7, approaches the spectrum-weighted moment of the inclusive cross section for production of π^0's,

$$Z_{p\pi^0}(0) = \int_0^1 x^{\alpha-2} f(x)\,\mathrm{d}x. \tag{40}$$

The moments are given in Table 1 for a range of spectral index.

The normalization constant for the spectrum of accelerated particles, which appears in Eqs. (35)-(37) is

$$K = \epsilon_p \times L_d \times \left(\int_{E_{\min}}^{E_p^{\max}} \frac{\mathrm{d}E_p}{E_p^{\alpha-1}} \right)^{-1}, \tag{41}$$

where ϵ_p is the efficiency for proton acceleration. This efficiency may be estimated by the solid angle, Ω_s, which the shock subtends at the pulsar (i.e. the solid angle over which the pulsar wind is confined):

$$\epsilon_p = \frac{\Omega_s}{4\pi} = \frac{1}{2}\{1 - [1 - (1 - \frac{r_s}{a})^2]^{1/2}\}, \tag{42}$$

which is only approximate because the shock is not spherical.

The total yield of photons in the target region (before reabsorption) for a thin target is

$$Y_\gamma(> E_\gamma) = \frac{\Delta X}{\lambda} N_\gamma(> E_\gamma), \tag{43}$$

where λ is the proton interaction length and ΔX the target thickness. For large pathlengths in the target region, ΔX in Eq. (43) is replaced by the nucleon attenuation length, $\Lambda = \lambda/(1 - Z_{NN})$, which takes account of the fact that a fast nucleon interacts several times before losing all its energy. The quantity Z_{NN} depends on α, and is included in Table 1. To estimate the magnitude of the photon flux seen by an observer at Earth, we next need to include a factor for the degree of beaming. This factor is $1/(\Delta\Omega\, d^2)$, where $\Delta\Omega$ is the solid angle into which the accelerated protons are emitted and d is the distance to Earth.

Finally, we must account for the duty cycle, $\Delta\phi_\gamma$, which represents the fraction of the orbital period during which photons are emitted toward the observer. There are large uncertainties in estimating this factor. In particular, the signal that is emitted from the source depends crucially on the extent to which photons are reabsorbed in the target region. If the target is the companion star, we get the Vestrand & Eichler (1982, 1984) picture in which photons are only emitted along lines of sight through the limb of the companion. This scenario results in a rather low average signal, though broadened somewhat if the proton source is extended over the whole region of interface between the companion wind and the pulsar

wind (see Fig. 1). At the other extreme, one can imagine a "leaky source" in which charged particles, after acceleration, are confined by diffusion in turbulent magnetic fields until they have lost all their energy in collisions, but the line of sight thickness of this target region is thin enough so that all produced photons escape. In this case the beaming factor must be assumed to have its maximum value of $\Delta\Omega = 4\pi$. An intermediate case occurs if the target is the companion star wind, compressed by its interaction with the pulsar wind (see Fig. 1). This, however, would be a thin target case ($\Delta X \sim 10^{-3}\,\mathrm{g\,cm^{-2}}$ for PSR 1957+20), with a relatively small yield of photons.

Assembling all the factors, the integral photon flux at Earth, averaged over the orbital period of the binary source, is

$$\Phi_\gamma(>E_\gamma) = \frac{\Delta\phi_\gamma}{\Delta\Omega\, d^2}\,\frac{\Delta X}{\lambda}\,\epsilon_\gamma\,\epsilon_p\,L_d, \tag{44}$$

where

$$\epsilon_\gamma = \frac{2}{\alpha(\alpha-1)}\,\frac{Z_{p\pi^0}(x_\gamma)}{(E_\gamma)^{\alpha-1}}\left(\int_{E_{\min}}^{E_p^{\max}}\frac{\mathrm{d}E_p}{(E_p)^{\alpha-1}}\right)^{-1}, \tag{45}$$

relates the photon spectrum to the parent spectrum that produces it. The factors in this equation have been grouped in this way for comparison with earlier estimates of the relation between the observed signal and luminosity at the source, especially the estimate of Hillas (1984) for Cygnus X-3. In addition, for $E_\gamma > 10^{14}$ eV, absorption of photons in the microwave background due to $\gamma\gamma \rightarrow e^+e^-$ must be accounted for. In the next section we use these ideas to estimate the signal from various sources.

V. Binary Sources of VHE and UHE Emission

There are known binary systems where acceleration in a pulsar wind shock could be occurring. The low mass X-ray binary Cygnus X-3 has been reported as a source of TeV and possibly PeV γ-rays at the 4.8 hr X-ray period (see Watson 1986 and Goodman 1989, for review). Both accretion and pulsar rotation have been suggested as the power source in this system, but the energy implied by the TeV and PeV γ-rays may favor (and perhaps require) a pulsar. There are also a number of binary systems known to contain spinning-down pulsars. In particular, the recent discovery of an eclipsing radio pulsar (Fruchter *et al.* 1988) has generated interest in the interaction of a pulsar wind with a companion star. We will discuss the application of the pulsar wind shock acceleration model to these systems and give predicted fluxes of high-energy γ-rays.

Table 2 lists binary pulsars with observed values of period P and period derivative $\dot{P}$, as well as some parameters for the Cyg X-3 system. Source distances (except for Cyg X-3) were determined from radio pulse dispersion measures assuming a mean interstellar electron density $\langle n_e \rangle = .03\,\mathrm{cm}^{-3}$. The companion masses in the binary pulsar systems are better determined than the Cyg X-3 companion mass. The value $0.5M_\odot$ for the Cyg X-3 companion listed in Table 2 is the largest main sequence star which will fit inside its Roche Lobe (Patterson 1984), but the actual mass could be larger if it is a Helium star. Also listed in Table 2 is the pulsar luminosity incident on the companion star, $L_* = \epsilon L_d$.

Since the predicted maximum proton acceleration energy in the pulsar wind shock model is proportional to the square root of the pulsar dipole luminosity, $E_p^{\max}$ may be determined for the case $r_s << 1 - r_*$ directly from the spin-down luminosity (if it is known), without having to know the pulsar period and magnetic field strength separately. In cases where the shock is close to the companion, the maximum proton energy will be reduced from this value, depending on the value of the shock radius. Determination of the shock radius, however, requires a model for the pulsar wind confinement, several of which were discussed in Section II. Which confinement model or models to apply to the sources in Table 2 is not clear. None of the sources has $L_* > L_{\mathrm{Edd}}$ required for an induced wind driven by radiation pressure (cf. Section II.b.1), although this is not certain in the case of Cyg X-3 as the companion mass could be less than $0.5M_\odot$. We could therefore use the thermal wind model, which does not require $L_* > L_{\mathrm{Edd}}$. According to Eqn (21), the shock solutions in this model are determined only by the wind terminal velocity $v_\infty/v_{\mathrm{esc}}$, which implicitly sets a value of $\dot{M}$. Eqn (22) sets an upper limit on v_∞ from the pressure balance requirement. There is also an upper limit on $\dot{M}$ from Eqn (3) for non-accreting sources like binary radio pulsars whose period and magnetic field strength are known. This upper limit on $\dot{M}$ is, strictly speaking, a limit on the neutron star accretion rate; the mass loss rate of the wind could be larger (but probably not much larger) if some of the mass escapes the system. The maximum values of $\dot{M}$ for the sources in Table 2 are listed in Table 3. We may therefore set a lower limit on v_∞ from Eqns (3) and (19). This gives a range of possible shock radii from the thermal wind model for the sources in Table 2. Given the uncertainty in the shock radius in these sources, we list the maximum proton acceleration energy in Table 3 without the geometric reduction factor, and compute gamma-ray fluxes using these values, but we will consider the above limits in a few of the sources.

We make the following assumptions for the parameters defined in Section IV to tabulate the π^0-decay photon flux from Eqn (44). Accelerated protons will escape downstream of the shock (*i.e.*, away from the pulsar) and so have a preferred direction. However, they will not be highly beamed, since the shock is an extended structure. We therefore take the proton solid angle $\Delta\Omega = 1$ sr. Within this solid angle, there are paths which encounter different thicknesses of target material, ranging from those going through the center of the companion star to those traversing less than 1 g cm^{-2}. The gamma-ray production efficiency increases with target thickness up to a maximum around 50 - 100 g cm^{-2}, and then decreases due to pair production attenuation. The peak gamma-ray signal will occur along those lines of sight where the gamma-ray production efficiency is maximum, where we can assume $\Delta X = \Lambda$ (thick target approximation). We also assume the proton acceleration efficiency, $\epsilon_p = \frac{1}{2}$ (its maximum value), and the gamma-ray duty cycle, $\Delta\phi_\gamma = 1$ (which effectively gives a peak flux). These are all multiplicative factors with which the predicted flux scales linearly. We show the results in Table 3 for two values of spectral index, α. Note that for steeper spectra the > 100 MeV flux is larger, but the > 1 TeV flux is much lower than for the flat spectrum. This is a simple consequence of the fact that for steeper spectra more of the luminosity is dumped into the low energy portion of the spectrum.

a) Cygnus X-3

Some previous estimates of the power required to explain signals from Cyg X-3 have been in excess of 10^{39} erg/s (Hillas 1984; Nagle, Gaisser and Protheroe 1988), and the required maximum proton energy is $E_p^{max} > 10^{16}$ eV. The fact that this luminosity exceeds the Eddington limit for steady accretion onto a neutron star ($\sim 10^{38}$erg s^{-1}), favors a model in which the power source is rotational energy release by a fast pulsar (Bignami *et al.* 1973, Vestrand and Eichler 1982). A period of 12.6 ms in TeV γ-rays from Cyg X-3 has been reported by the Durham group (Chadwick *et al.* 1985). The periodicity, not yet confirmed by other groups (Ramana-Murthy 1989), appears sporadically in the signal and measurements of changes in this period over 7 years give a period derivative $\dot{P} \approx 3 \times 10^{-14}$ s s^{-1} (Turver 1989, private comm.). These values of P and $\dot{P}$ give a magnetic field strength of 6×10^{11} G and dipole luminosity 6×10^{38}erg s^{-1}.

It is interesting that the value of $\dot{M} < 9.3 \times 10^{18}$ g s^{-1} derived from Eqn (3) using the values of P and $\dot{P}$ reported by Chadwick *et al.* (1985) from TeV observations is just under

the upper limit, $\dot{M} < 10^{20}\,\mathrm{g\,s^{-1}}$, on the Cyg X-3 system mass loss from the observed orbital period derivative (Bonnet-Bidaud and Van der Klis 1981). Since the shock location and maximum proton acceleration energy depend on the pulsar dipole luminosity, we do not need to know the pulsar period and magnetic field separately in applying the pulsar wind shock model to the Cyg X-3 system. We do need to know or assume values for the binary orbital period, companion mass and radius, separation and distance. The values we take for these parameters are shown in Table 2.

The maximum proton acceleration energy, $E_p^{\max}$, scales with $L_d^{1/2}$. Assuming the dipole luminosity $L_d = 6 \times 10^{38}\mathrm{erg\,s^{-1}}$ implied by the values of P and $\dot{P}$ observed by Chadwick *et al.* (1985) gives $E_p^{\max} = 3 \times 10^4$ TeV. Using the formula in Eqn (44) for two values of proton spectral index α, the predicted flux of $>$ TeV γ-rays from the source is $3.4 \times 10^{-9}\mathrm{ph\,cm^{-2}\,s^{-1}}$ for $\alpha = 2$ and $3.0 \times 10^{-11}\mathrm{ph\,cm^{-2}\,s^{-1}}$ for $\alpha = 2.7$. The predicted flux of $>$ 100 MeV γ-rays is $3.4 \times 10^{-5}\mathrm{ph\,cm^{-2}\,s^{-1}}$ for $\alpha = 2$ and $1.9 \times 10^{-4}\mathrm{ph\,cm^{-2}\,s^{-1}}$ for $\alpha = 2.7$. In order to compare with phase-averaged observed fluxes, our peak flux predictions should be multiplied by the observed 4.8 hr duty cycle, $\Delta\phi_\gamma \approx 0.1$. With the assumptions made, the $\alpha = 2$ TeV flux predicted for Cygnus X-3 is greater than has been observed (Dowthwaite *et al.* 1984). The $>$ 100 MeV fluxes tabulated are consistent with the SAS 2 measurement (SAS 2 is 1.1×10^{-5} above 35 MeV, Lamb *et al.* 1977, Fichtel *et al.* 1987 and earlier references therein), but are somewhat above the upper limit from the COS B observations (Hermsen *et al.*, 1987), which is about 10^{-6} for $>$ 70 MeV photons. The primary reason that the predicted fluxes are high in the pulsar wind acceleration model is because of the much higher efficiency for generating a gamma-ray signal from Cyg X-3 than the Vestrand-Eichler model. Since the accelerator is closer to the target material, a greater fraction of the accelerated protons can interact to produce gamma-rays. Consequently, the fraction of the pulsar spin-down power which is converted to accelerated protons need not be as large. Alternatively, emission from the source may be sporadic at the highest energies.

Applying the thermal wind model to the Cyg X-3 system, we find that there is no range in wind terminal velocity which, as discussed above, gives a solution to Eqn (8) for the shock radius and satisfies the limit on $\dot{M}$. Physically, the ram pressure of an induced thermal wind with $\dot{M} < \dot{M}_{\max}$ (at least with the choices for parameter values made in Section II.B.2) is not large enough to stand off the pulsar wind above the companion surface. Either the parameter values chosen are not appropriate or the thermal wind model of Cheng (1989) does

not work for this system, possibly because it is close to the Eddington limit. Alternatively, it is possible that only part of the pulsar wind exerts pressure on the companion star wind (Rasio, Shapiro and Teukolsky 1989). In any case, because Cyg X-3 is a close binary the shock radius would be of the order of $r_s/a \approx 0.5$ and the geometrical reduction factor in Eqn (33) for $E_p^{\max}$ is close to unity.

b) Binary Pulsars

We have calculated the maximum proton energy in the pulsar wind acceleration model for nine known binary radio pulsars, listed in Table 2 with their period P, period derivative $\dot{P}$, orbital period P_b, companion mass M_c and distance d (cf. Dewey *et al.* 1986). Table 3 gives the values of $\dot{M}_{\max}$ and $E_p^{\max}$, as well as the predicted γ-ray fluxes from Eqn (44) for $\alpha = 2$ and $\alpha = 2.7$. Several sources have predicted fluxes of > 100 MeV γ-rays which are above the sensitivity threshold of $5 \times 10^{-8}\,\mathrm{ph\,cm^{-2}\,s^{-1}}$ of the EGRET detector (Kanbach *et al.* 1988) on the Gamma-Ray Observatory (GRO). Because of the dependence of maximum proton energy on pulsar luminosity, these are also the systems capable of producing γ-rays above 1 TeV. One of these, PSR1957+20, is the eclipsing millisecond pulsar which may be evaporating its companion by means of an induced wind (Phinney *et al.* 1988, Kluzniak *et al.* 1988, Cheng 1989). A mass loss rate of $\dot{M} \approx 10^{16}\,\mathrm{g\,s^{-1}}$ is sufficient to evaporate it completely in the pulsar's lifetime. Another system, PSR1855+09, contains a 5 ms pulsar and is relatively nearby, giving a predicted flux > 100 MeV well above EGRET sensitivity (for the assumptions we have made).

Since the r_s solutions in the thermal wind model are parameterized by the wind terminal velocity, we must specify a value of v_∞ in the solution for r_s. Since $r_s/a << 1$ in all of these systems, the upper limit on v_∞ from Eqn (22) is around $0.29\,v_{\rm esc}$. In several systems, notably PSR1913+16, the companion is probably another neutron star, which would not be expected to have a wind. In that case, the magnetic pressure of the neutron star companion or ram pressure of another pulsar wind would balance the pulsar wind, with the shock location determined by Eqn (23).

In the case of the eclipsing pulsar PSR1957+20, it is not clear whether a pulsar induced thermal wind is capable of supporting the pulsar wind above the stellar surface. The mass loss rate in the X-ray heated thermal wind model, using Eqn (17), is $\dot{M} \simeq 6 \times 10^{13}\,\mathrm{g\,s^{-1}}$ (Emmering and London 1989), assuming $v_\infty = v_{\rm esc}$. The solution for the shock location

from Eqn (18) gives $r_s/a \simeq .985$, which is inside the star. In the model of Cheng (1989), a value $(v_\infty/v_{esc}) = 0.1$ puts the shock at the observed eclipse radius, $r_s/a \approx 0.6$. The formula in Eqn (10) gives $1 - r_s/a \approx 9.3\,(r_*/a)$ for $(v_\infty/v_{esc}) = 0.1$ when $A_w >> 1$, so in this case the shock stands off about 9.3 stellar radii from the companion. This value of r_s/a reduces E_p^{max} only slightly from the value in Table 3 to 250 TeV, which will not change the > 1 TeV flux estimate. However, $(v_\infty/v_{esc}) = 0.1$ gives a value $\dot{M} = 6 \times 10^{17}\,g\,s^{-1}$ from Eqn (19), which is much larger than the rate (given in Table 3) at which the pulsar would begin to accrete mass. Increasing (v_∞/v_{esc}) to 0.5 would satisfy the limit on $\dot{M}$, but the induced wind is then barely able to stand off the pulsar wind above the companion surface. In this case, E_p^{max} would be reduced to 20 TeV, with a resulting decrease in the > 1 TeV γ-ray flux by a factor of 3 for $\alpha = 2$.

In the case of PSR1855+09, a value of $(v_\infty/v_{esc}) > .057$ is required to keep the induced $\dot{M}$ in the thermal wind model below $\dot{M}_{max}$. However, we require $(v_\infty/v_{esc}) < .29$ for pressure balance with the pulsar wind, so there is a range of allowed solutions. Even in the most favorable case, $\dot{M} = \dot{M}_{max}$, the solution for the shock radius is then $r_s/a = 0.95$ and E_p^{max} is reduced to only 4 TeV, lowering the predicted flux to 0.1% of the value in Table 3.

VI. Discussion

We have proposed a model for particle acceleration in VHE and UHE γ-ray sources which contain rapidly spinning, non-accreting pulsars. Considering the physics of the first-order Fermi mechanism at the pulsar wind shock, acceleration to energies above 10^{17} eV is in principle possible (e.g. if the source contains a 10 ms pulsar with a 10^{12} G magnetic field). Furthermore, the power source is the pulsar spin-down, which could supply superEddington luminosities in accelerated particles. Models for UHE sources in which the power source is accretion have a luminosity limit of $L < 2 \times 10^{38}\,erg\,s^{-1}(R_o/R)$, where R is the radius at which the accretion energy is converted particle energy. These models also have difficulty accelerating particles to the energies needed to produce UHE γ-rays (see Harding 1989 for review). The pulsar wind model is able to generate the combination of UHE γ-ray emission and possibly superEddington luminosity of Cyg X-3. In addition, the accelerator-target configuration in this model may be more favorable, so that the power required to produce a given signal is not so severe. This acceleration model would not apply to sources like Her X-1 and Vela X-1, which have been detected at VHE and UHE energies, but are known to

be accreting neutron stars. In these cases though, the power available through accretion is sufficient to account for the observed γ-ray fluxes.

If confined pulsar winds result in acceleration of particles, then some binary pulsars which have been detected by their radio pulses could be γ-ray sources. Recently, emission at TeV energies has been reported by von Ballmoos *et al.* (1989) and de Jager *et al.* (1989) from two binary pulsars. Data from PSR1957+20, folded with the 9 hr orbital period, shows a peak in the phase plot at the position of the $L4$ Lagrange point. The reported flux above 2 TeV is 1.1×10^{-9} photons $cm^{-2} s^{-1}$, much higher than our predicted fluxes in Table 3. This difference is due to the small γ-ray solid angle of $\Delta\Omega \approx .009$ derived by von Ballmoos *et al.* (1989) from the width of the phase peak ($\Delta\phi_\gamma = .018$), whereas we have taken $\Delta\Omega = 1$ sr to compute the fluxes in Table 3. A peak at the $L4$ position in the orbital phase plot of PSR1957+20 may also have been seen at > 100 MeV in COS-B data (von Ballmoos *et al.* 1989). A TeV signal was also reported by de Jager *et al.* (1989) at the 5.4 ms pulsar period of PSR1855+09 at a marginal significance level. Signals which are observed to be pulsed at the pulsar period, however, must originate from acceleration near or within the pulsar magnetosphere and would not be expected from particles accelerated at the pulsar wind shock.

The currently favored model for the origin of binary systems containing short period pulsars is spin up by an accretion disk (Alpar *et al.* 1982). The accretion spin-up period depends on the neutron star magnetic field in this model, with a spin-up period in the 10 ms range requiring a field around 10^9 Gauss. This evolution model accounts quite well for the observed binary pulsars, which all have low magnetic fields. The high luminosity implied by the observed Cyg X-3 gamma-ray flux requires not only a short period but also a high magnetic field, incompatible with an accretion spin-up evolution. A fast pulsar as the power source in Cyg X-3 would therefore have originated in a relatively recent supernova explosion that occurred within the pulsar spin-down time of 7000 yr. Confined pulsar wind sources of this type would be more rare than the accretion spun-up binary pulsars, which have ages of around 10^8 yr.

In this paper, we have examined pressure balance only along the line between the pulsar and the companion. In other directions, the balance point, and thus the shock location, would be further from the companion. The details of the particle acceleration and gamma-ray production (predicted light curves, etc.) will require a full solution to the pressure balance

and the shape of the pulsar wind shock. In addition, such a solution may allow asymmetric pulsar-induced winds in cases where there is no pressure balance above the stellar surface. Thus, a thermal wind ram pressure too low to support the pulsar wind above the surface facing the pulsar does not altogether prevent ablation from the limb of the star.

We also have not addressed the question of the source of protons which are accelerated at the shock. One possible source of protons is the pulsar wind, which in most models contains only electrons and positrons, but could conceivably carry some ions. Another possibility is that some of the material from the companion star wind or atmosphere may mix into the pulsar wind just downstream of the shock, through Rayleigh-Taylor instabilities at the contact discontinuity. Such a mechanism for mixing has been investigated in the context of a pulsar wind confined by a supernova remnant (Gaisser *et al.* 1989, Harding *et al.* 1989). In the binary system, though, the distance of the pulsar wind shock to the contact discontinuity is not as easily determined, since it would require a steady-state solution for the flow of the pulsar wind around the companion.

We thank A. Cheng, D. C. Ellison, R. London, R. J. Protheroe, L. Rawley, M. Ruderman, and M. Tavani for helpful and stimulating discussions. We also acknowledge the Aspen Center for Physics where this work was initiated.

REFERENCES

Alpar, M. A., Cheng, A. F., Ruderman, M. A. and Shaham, J. 1982, *Nature*, **300**, 728.

Arons, J. 1981, in *IAU Symposium 94: Origin of Cosmic Rays*, eds. G. Setti, G. Spada and A. W. Wolfendale (Reidel, Dordrecht), p. 175.

Auriemma, G., Gaisser, T. K. and Lipari, P. 1988, *Nuovo Cimento*, **102B**, 583.

Berezinsky, V. S. and Kudryavtsev, V. A. 1989, *Ap. J.*, in press.

Bignami, G. F., Maraschi, L. and Treves, A. 1973, *Astron. Astrophys.*, **55**, 155.

Blandford, R. D. and Ostriker, J. P. 1978, *Ap. J. Letters*, **221**, L29.

Bonnet-Bidaud, J. M. and Van der Klis, M. 1981, *Astr. Ap.*, **101**, 299.

Castor, J. I., Abbott, D. C. and Klein, R. I. 1975, *Ap. J.*, **195**, 157.

Cesarsky C. J. and Montmerle, T. 1983, *Space Sci. Rev.*, **36**, 173.

Chadwick, P. M. *et al.* 1985, *Nature*, **318**, 642.

Cheng, A. F. 1983, *Ap. J.*, **275**, 790.

Cheng, A. F. 1989, *Ap. J.*, **339**, 291.

Davies, R. E. and Pringle, J. E. 1981, *M.N.R.A.S.*, **196**, 209.

de Jager, O. C. *et al.* 1989, *Nuclear Phys. B (Proc. Supp.)*, in press.

Dewey, R. J. *et al.* 1986, *Nature*, **322**, 712.

Dowthwaite *et al.* 1984, *Nature*, **309**, 691.

Drury, L. O'C. 1983, *Rep. Prog. Phys.*, **46**, 973.

Eichler, D. and Ko, Y. 1988. *Ap. J.*, **328**, 179.

Eichler, D. and Vestrand, W. T. 1984, *Nature*, **307**, 613.

Ellison, D. C. and Eichler, D. 1984, *Ap. J.*, **286**, 691.

Ellison, D. C., Jones F. C. and Reynolds, S. P. 1990, *Ap. J.*, submitted.

Emmering, R. T. and Chevalier, R. A. 1987, *Ap. J.*, **321**, 334.

Emmering, R. T. and London, R. A. 1989, in preparation.

Fichtel, C. E., Thompson, D. J. and Lamb, R. C. 1987, *Ap. J.*, **319**, 362.

Fruchter, A. S., Stinebring, D. R. and Taylor, J. H. 1988, *Nature*, **333**, 237.

Gaisser, T. K. 1988, in *Proc. Snowmass Summer Workshop*, in press.

Gaisser, T. K., Harding, A. K. and Stanev, T. 1987, *Nature*, **329**, 314.

Gaisser, T. K., Harding, A. K. and Stanev, T. 1989, *Ap. J.*, **345**, 423.

Goldreich, P. and Julian, W. H. 1969, *Ap. J.*, **157**, 869.

Goodman, J. 1989, *Nuclear Physics B (Proc. Supp.)*, in press.

Harding, A. K. 1989, *Nuclear Phys. B (Proc. Supp.)*, in press.

Harding, A. K., Mastichiadis, A. and Protheroe, R. J. 1989, in *Proc. of 21st Intl. Cosmic Ray Conf.*, **2**, 226.

Hermsen, W. *et al.* 1987, *Astron. Astrophys.*, **175**, 141.

Hillas, A. M. 1984, *Nature*, **312**, 50.

Jokipii, J. R. 1987, *Ap. J.*, **313**, 842.

Kanbach, G. *et al.* 1988, *Space Sci. Rev.*, **49**, 69.

Kennel, C. F. and Coroniti, F. V. 1984a, *Ap. J.*, **283**, 694.

Kennel, C. F. and Coroniti, F. V. 1984b, *Ap. J.*, **283**, 710.

Kirk, J. G. and Schneider, P. 1987, *Ap. J.*, **315**, 425.

Kluzniak, W., Ruderman, M. A., Shaham, J. and Tavani, M. 1988, *Nature*, **334**, 225.

Kulkarni, S. R. and Hester, J. J. 1989, *Nature*, **335**, 801.

Lagage, P. O. and Cesarsky, C. J. 1983, *Astr. Ap.*, **125**, 249.

Lamb. R. C., Fichtel, C. E., Hartman, R. C., Kniffen, D. A. and Thompson, D. J. 1977, *Ap. J. Letters*, **212**, L63.

London, R., McCray, R. and Auer, L. H. 1981, *Ap. J.*, **243**, 970.

London, R. A. and Flannery, B. P. 1982, *Ap. J.*, **258**, 260.

Mihalis, D. 1978, *Stellar Atmospheres* (San Francisco: Freeman).

Nagle, D. E., Gaisser, T. K. and Protheroe, R. J. 1988, *Ann. Rev. Nucl. Part. Sci.*, **38**, 609.

Ostriker, J. P. and Gunn, J. E. 1969, *Ap. J.*, **157**, 1395.

Patterson, J. 1984, *Ap. J. Suppl.*, **54**, 443.

Peacock, J. A. 1981, *M.N.R.A.S.*, **196**, 135.

Phinney, E. S., Evans, C. R., Blandford, R. D. and Kulkarni, S. R. 1988, *Nature*, **333**, 832.

Protheroe, R. J. 1983, *Nature*, **310**, 296.

Ramana-Murthy, P. V. 1989, *Nuc. Phys. B (Proc. Supp.)*, in press.

Rasio, F. A., Shapiro, S. L. and Teukolsky, S. A. 1989, *Ap. J.*, **342**, 934.

Rees, M. J. and Gunn, J. E. 1974, *M.N.R.A.S.*, **167**, 1.

Ruderman, M. A., Shaham, J. and Tavani, M. 1989, *Ap. J.*, **336**, 507.

Ruderman, M. A., Shaham, J., Tavani, M. and Eichler, D. 1989, *Ap. J.*, **343**, 292.

Shakura, N. I. and Sunyaev, R. A. 1973, *Astron. Ap.*, **24**, 337.

Sturrock, P. A. 1971, *Ap. J.*, **164**, 529.

Vestrand, W. T. and Eichler, D. 1982, *Ap. J.*, **261**, 251.

Von Ballmoos, P. *et al.* 1989, *Proc. of GRO Science Workshop*, p. 4-182.

Watson, A. A. 1986, in *Proc. 19th Intl. Cosmic Ray Conf.*, **9**, 111.

Table 1

Parameters for Photon Production

α	2.0	2.2	2.4	2.6	2.8
Z_{NN}	0.41	0.37	0.34	0.31	0.29
$Z_{N\pi^0}$ (includes 6% η)	0.17	0.092	0.066	0.048	0.036

Table 2

Binary Pulsar Parameters

PSR	P (ms)	Log(P)	P_b (days)	M_c ($M_\odot$)	a (cm)	d (kpc)	L_d (erg/s)	L_* (erg/s)
1913+16	59	-17.1	0.32	1.4	1.9 (11)	4.33	1.58 (33)	7.1 (28)
0655+64	195.6	-18.2	1.03	1	4.0 (11)	0.27	3.45 (30)	4.5 (25)
1831-00	520.9	-17	1.81	0.1	5.0 (11)	3.13	2.90 (30)	1.1 (26)
1855+09	5.4	-19.8	12.33	0.3	1.9 (12)	0.44	4.12 (33)	5.6 (27)
2303+46	1066.4	-15.4	12.34	2	2.4 (12)	2.0	1.34 (31)	3.2 (24)
1953+29	6.1	-19.5	117.35	0.3	8.4 (12)	2.92	5.71 (33)	3.8 (26)
0820+02	864.9	-16	1232.4	0.3	4.0 (13)	0.79	6.33 (30)	1.8 (22)
1957+20	1.61	-19.9	0.381	0.02	1.7 (11)	1.0	1.24 (35)	1.2 (32)
1620-26	11.1	-18.1	191.44	0.35	1.2 (13)	2.1	2.38 (34)	7.3 (26)
CYG X-3	12.6	-13.5	0.2	0.5	1.2 (11)	10	6 (38)	2.1 (37)

Table 3

Gamma-Ray Flux from Binary Pulsars

PSR	M_{max} (g/s)	r_*/a	E_p^{max} (TeV)	$\Phi_\gamma(>1\text{TeV})$ (ph cm^{-2} s^{-1})		$\Phi_\gamma(>100\text{MeV})$ (ph cm^{-2} s^{-1})	
				$\alpha = 2.0$	$\alpha = 2.7$	$\alpha = 2.0$	$\alpha = 2.7$
1913+16	2.0 (13)	1.34 (-2)	50.3	4.5 (-14)	2.5 (-16)	7.3 (-10)	2.6 (-9)
0655+64	2.1 (11)	7.25 (-3)	2.35	—	—	5.9 (-10)	1.6 (-9)
1831-00	2.8 (11)	1.25 (-2)	2.15	—	—	3.6 (-12)	9.2 (-12)
1855+09	4.1 (13)	2.32 (-3)	81.2	1.2 (-11)	1.0 (-13)	1.6 (-7)	6.8 (-7)
2303+46	1.9 (12)	9.78 (-4)	4.64	—	—	3.7 (-11)	1.0 (-10)
1953+29	6.0 (13)	5.17 (-4)	95.6	4.2 (-13)	3.3 (-15)	5.5 (-9)	2.2 (-8)
0820+02	7.9 (11)	1.08 (-4)	3.18	—	—	1.2 (-10)	3.2 (-10)
1957+20	6.8 (14)	6.17 (-2)	445	8.9 (-11)	6.2 (-13)	8.9 (-7)	3.9 (-6)
1620-26	3.4 (14)	3.51 (-4)	195	3.6 (-12)	2.7 (-14)	4.2 (-8)	1.7 (-7)

FIGURE CAPTIONS

Figure 1 - Schematic view of pulsar wind shock formation in a binary system for the case of confinement by the companion star wind.

Figure 2 - Distance of the pulsar wind shock from the pulsar vs. companion radius for the general case of confinement by a companion star wind. Curves are labeled with values of the dimensionless parameter, A_w, defined in Eqn (11). The curved right-hand boundary of the solutions is where $r_s = a - r_*$.

Figure 3 - Distance of the pulsar wind shock from the pulsar vs. companion radius for the case of confinement by a companion star wind driven by radiation pressure. Curves are labeled with values of $P_{\rm ms} B_{12}^{-1/2}$.

Figure 4 - Distance of the pulsar wind shock from the pulsar vs. companion radius for the case of confinement by a companion star thermal wind. Curves are labeled with values of $v_\infty / v_{\rm esc}$.

Figure 5 - Distance of the pulsar wind shock from the pulsar vs. companion radius for the case of confinement by a companion star magnetosphere. Curves are labeled with values of the dimensionless parameter, $\log_{10}(A_m)$, defined in Eqn (24).

Figure 6 - Limits on $L_{38} \equiv L_d / 10^{38}\,{\rm erg\,s^{-1}}$ and companion radius to binary separation ratio required for proton acceleration to energies above 10 and 10^4 TeV in a pulsar wind shock, for the case of pressure balance in the stellar atmosphere.

Figure 7 - Relative efficiency of π^0-decay photon production for power law proton spectra with index $\alpha = 2.0, 2.2, 2.4, 2.6, 2.8$. The function $Z_{p\pi^0}(x_\gamma)$ is defined in Eqns (38) and (40). The quantity $x_\gamma \equiv E_\gamma / E_p^{\rm max}$.

ALICE K. HARDING: Code 665, NASA/Goddard Space Flight Center, Greenbelt, MD 20771.

T. K. GAISSER: Bartol Research Institute, University of Delaware, Newark, DE 19716.

*U.S. GOVERNMENT PRINTING OFFICE: 1990--262-934/28059

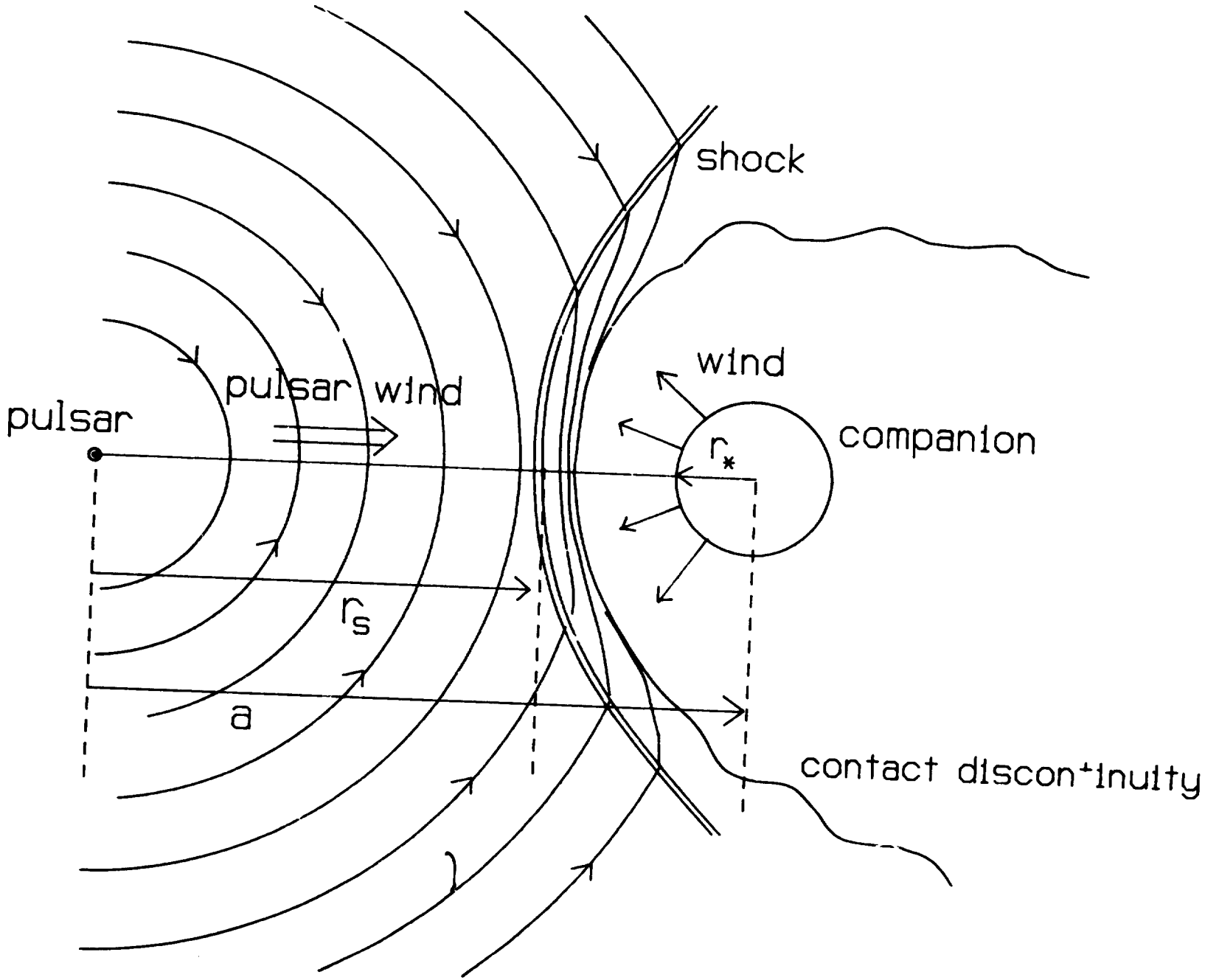
shock
wind
pulsar wind
pulsar
companion
r_*
r_s
a
contact discontinuity

Figure 1

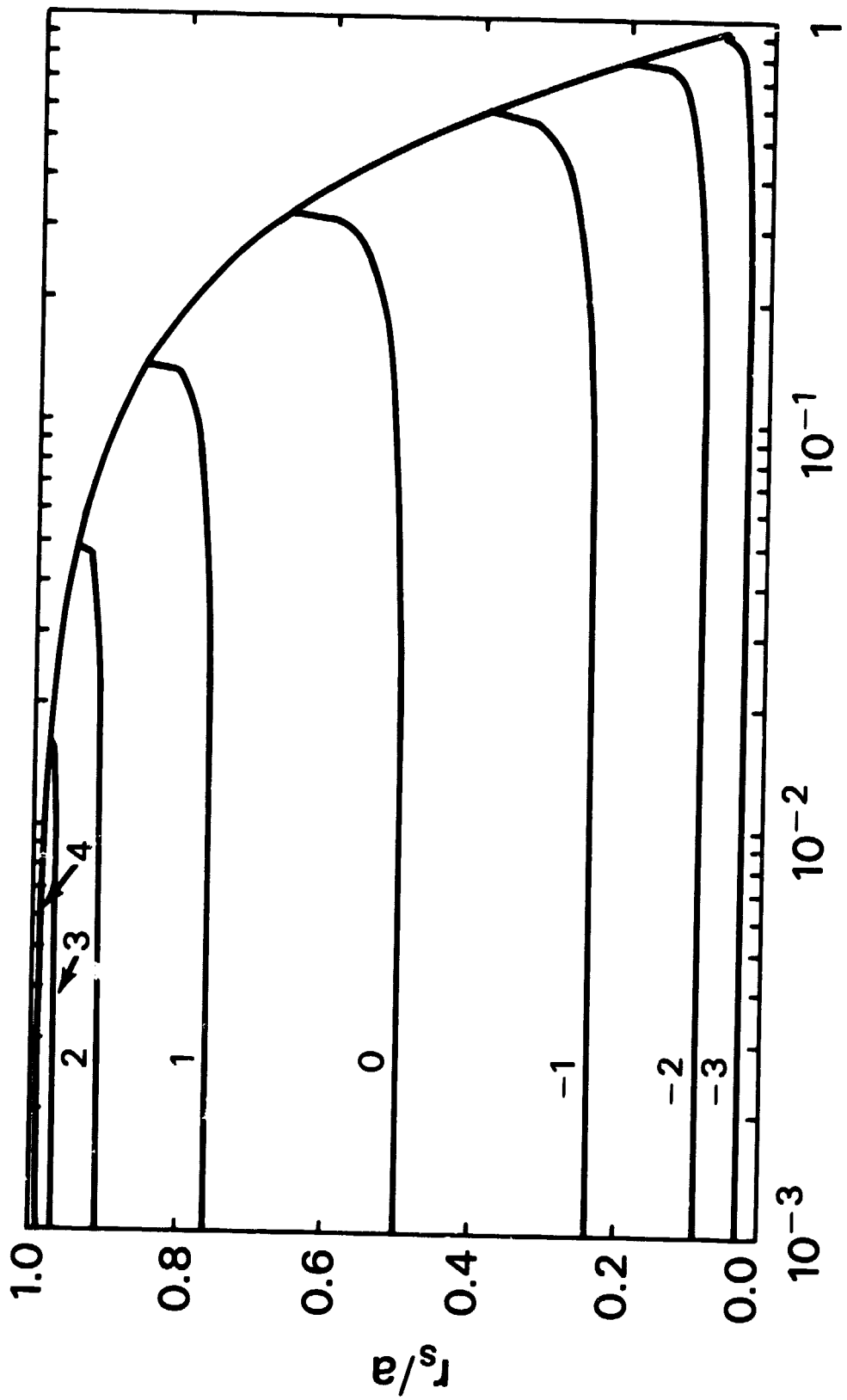

Figure 2

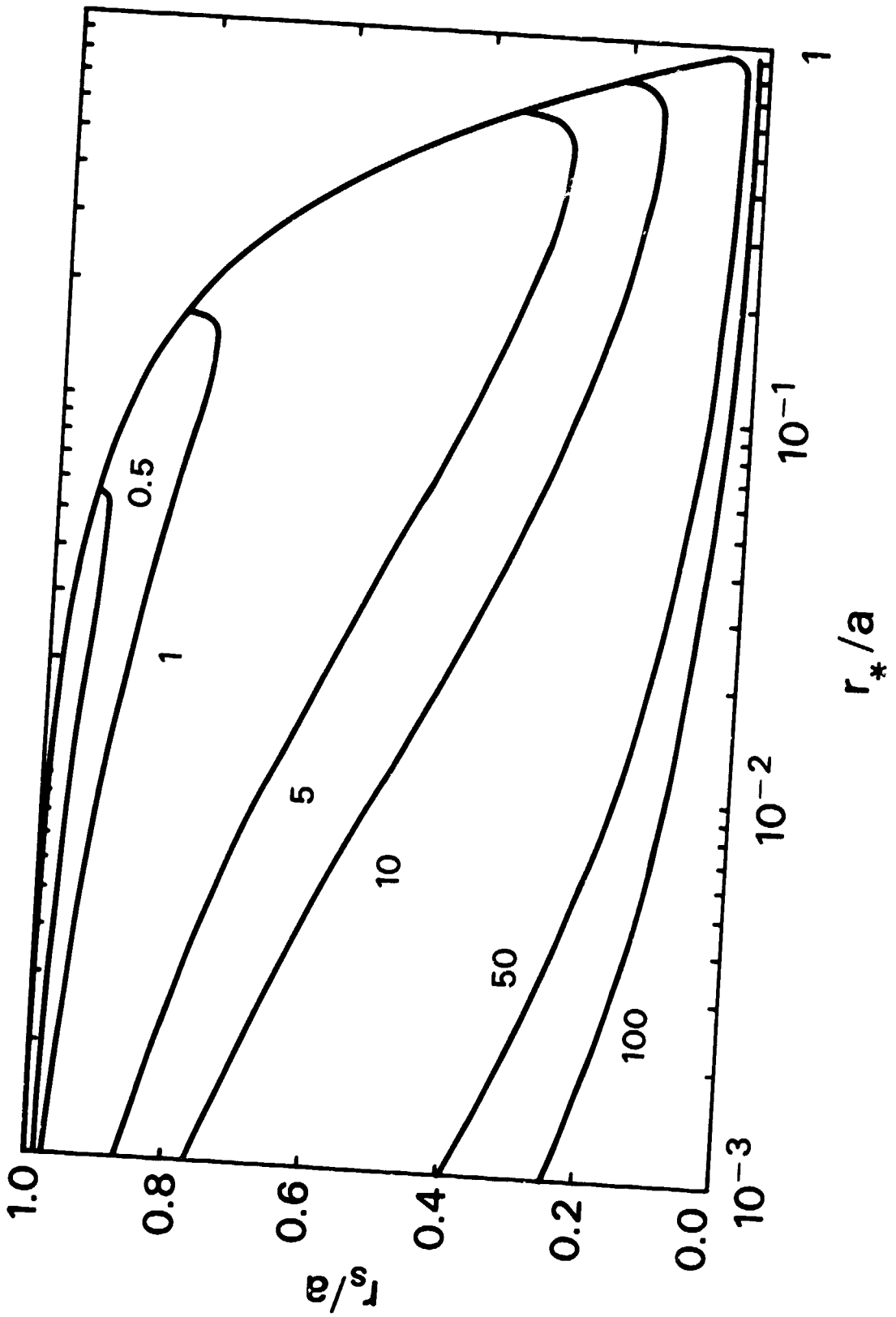

Figure 3

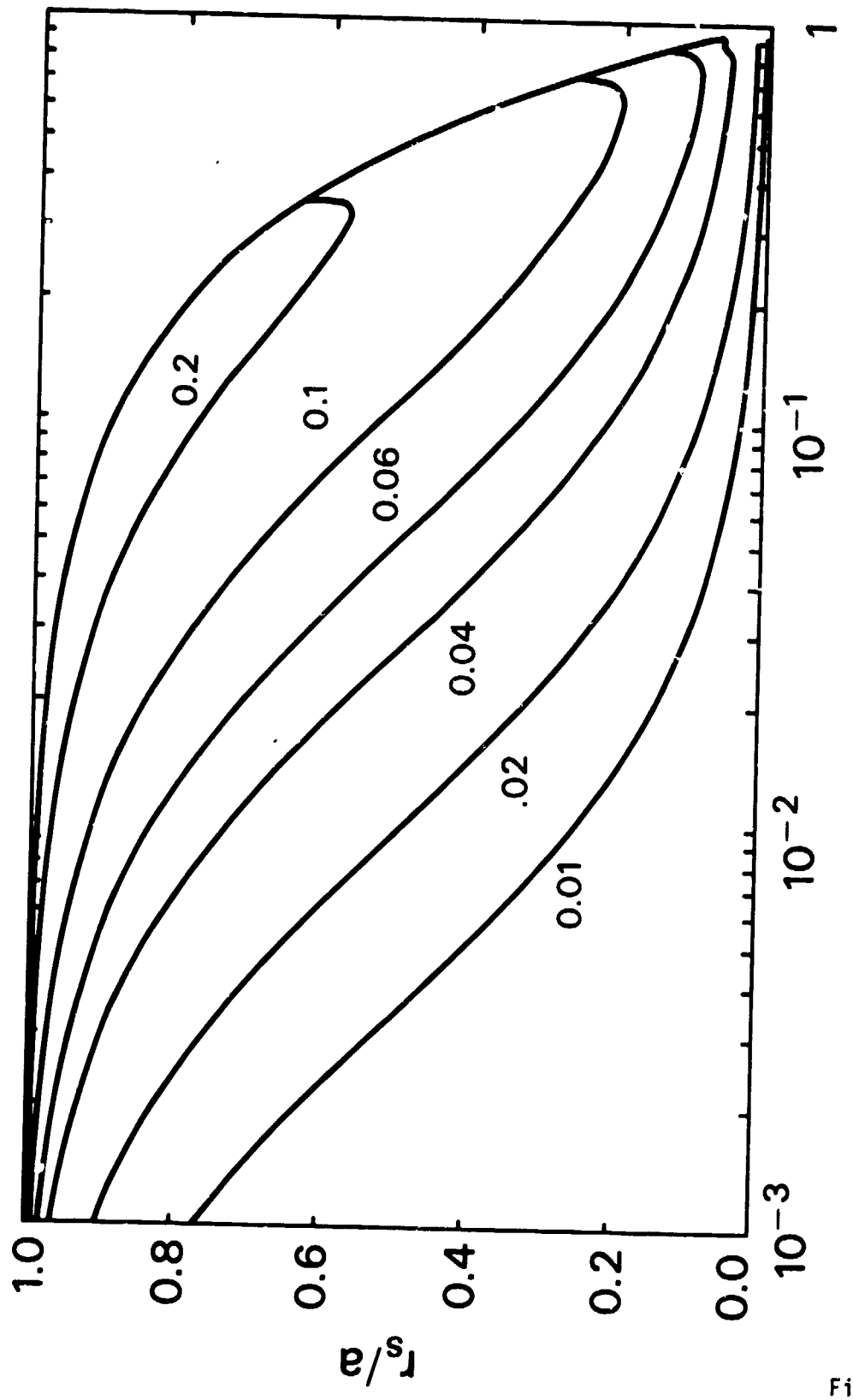

Figure 4

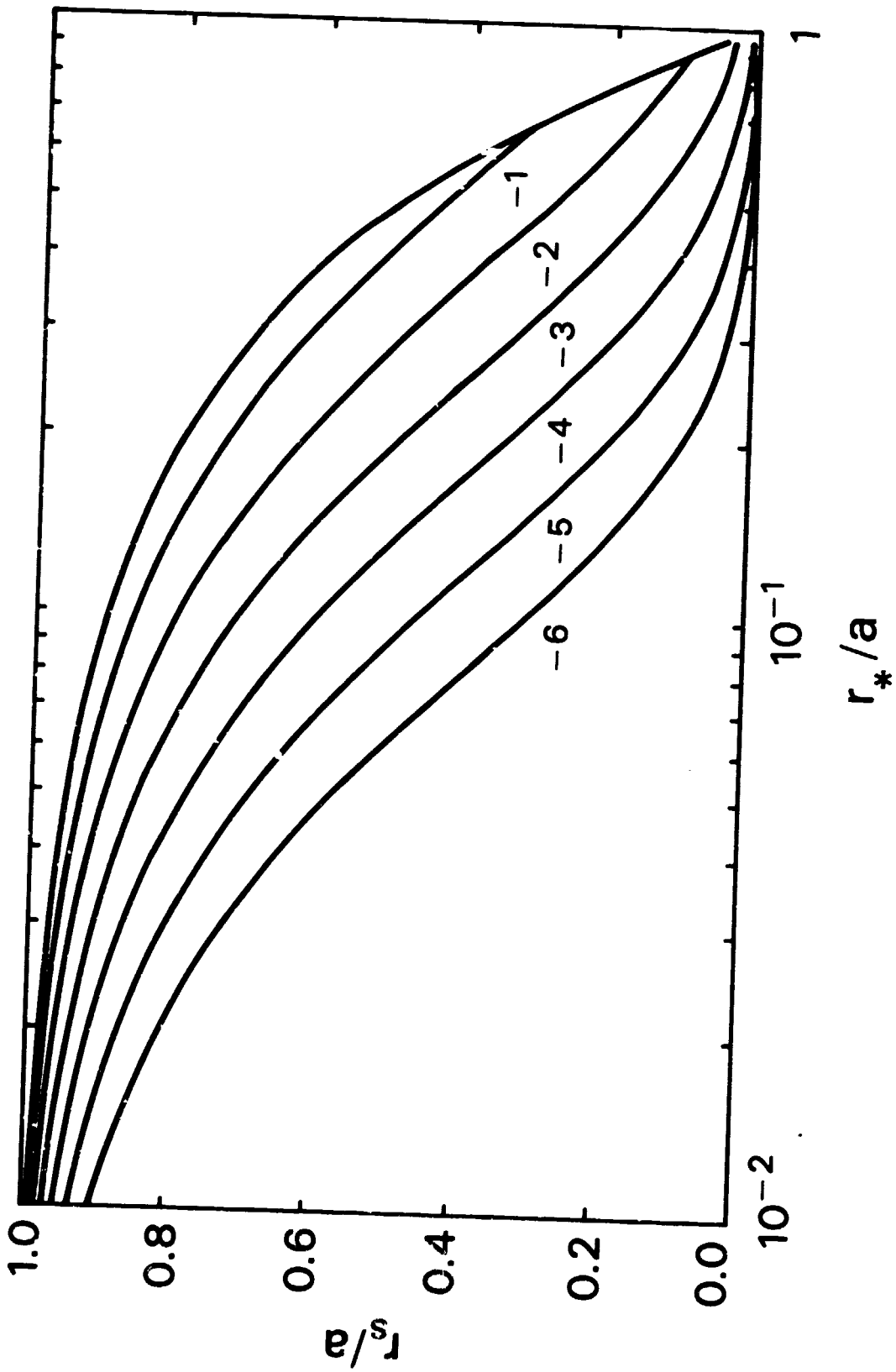

Figure 5

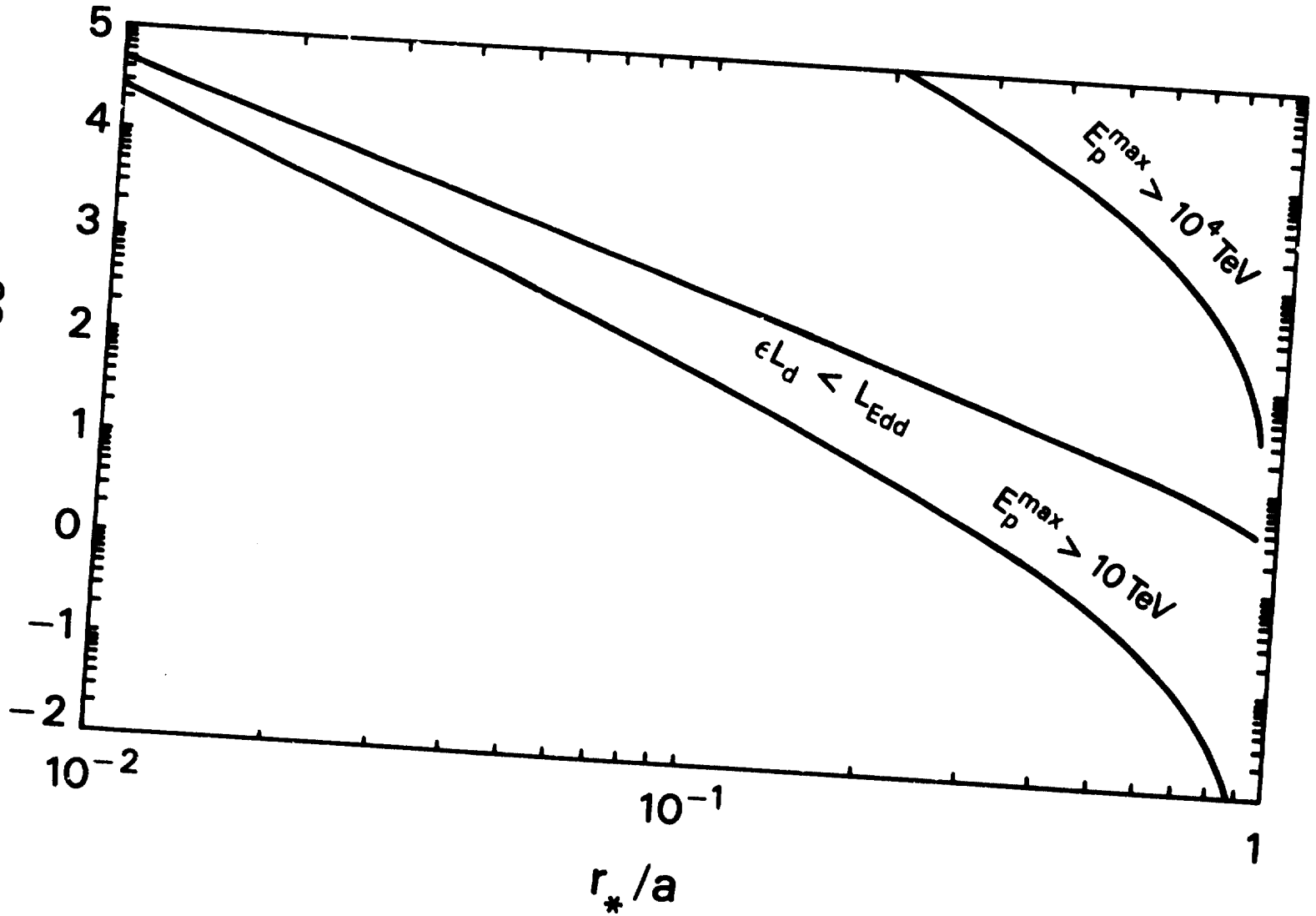
5
4
3
2
1
0
−1
−2
log (L38)
10^{-2}
10^{-1}
1
r_*/a
$E_p^{max} > 10^4$ TeV
$\epsilon L_d < L_{Edd}$
$E_p^{max} > 10$ TeV

Figure 6

α=2.8
α=2.0
1.0
0.9
0.8
0.7
0.6
0.5
0.4
0.3
0.2
0.1
$Z_{pmo}(X_\gamma)/Z_{pmo}(0)$
10^{-1}
10^{-2}
X_γ

Figure 7